The Thermodynamic Properties of Propane: From *p*-ρ-*T* to the Equation of State[1]

MARK O. MCLINDEN, *Chemical Engineer, Physical and Chemical Properties Division, National Institute of Standards and Technology, Boulder, Colorado, USA.* *markm@boulder.nist.gov*
ERIC W. LEMMON, *Mechanical Engineer, Physical and Chemical Properties Division, National Institute of Standards and Technology, Boulder, Colorado, USA.* *ericl@boulder.nist.gov*

ABSTRACT

The *p*-ρ-*T* behavior of high-purity (99.999 %) propane was measured from 265 K to 500 K with pressures to 36 MPa using a two-sinker densimeter. The measurements extend from low-density vapor to compressed liquid states, and the near-critical region was covered extensively. Vapor pressures from 265 K to 369 K have also been measured. The apparatus is described and the uncertainties in the measurements are discussed. These data, together with new heat capacity data measured at NIST and carefully selected literature data, have been used to develop an equation of state (EOS) valid over the entire fluid region from the triple point temperature of 85.528 K to 520 K with pressures to 1000 MPa. The equation is written in terms of the Helmholtz energy and includes special terms to describe the critical region. This EOS is among the most accurate for any fluid, and the new data were crucial in its development. The EOS exhibits proper extrapolation behavior to high temperatures and pressures. It will serve as a reference fluid for the fitting of simpler models for fluids with limited data.

1. INTRODUCTION

Propane is among the refrigerants with zero ozone depletion potential and low global warming potential experiencing increased interest and use. It is also an excellent reference fluid for the development of thermophysical property models. Extensive property measurements have been published for propane; these are summarized by Lemmon *et al.* (2005). Two of the more commonly used equations of state are Younglove and Ely (1987) and Miyamoto and Watanabe (2000). While propane has been well-studied, its properties are not as well-known as generally assumed. The purposes of the current project are to provide new data of the highest accuracy and to develop a comprehensive equation of state. These will illustrate the current state of the art.

2. EXPERIMENTAL

2.1 Apparatus Description

Measurements were carried out in a two-sinker densimeter. This instrument is detailed elsewhere (McLinden and Lösch 2005), but a brief description is given here. The basic principle is an Archimedes (buoyancy) technique where two sinkers of the same mass, surface area, and surface material, but very different volumes, are weighed separately while immersed in a fluid of unknown density. The fluid density ρ is given by

$$\rho = \frac{(m_1 - W_1) - (m_2 - W_2)}{(V_1 - V_2)} \,, \tag{1}$$

where *m* is mass, *W* is the balance reading, *V* is volume, and the subscripts refer to the two sinkers. The main advantage of the two-sinker method is that adsorption onto the surface of the sinkers, systematic errors in the weighing, and other effects that reduce the accuracy of most buoyancy techniques cancel. The sinkers have a mass of 60 g each and are fabricated of tantalum and titanium; both are gold plated.

A magnetic suspension coupling transmits the gravity and buoyancy forces on the sinkers across a pressure barrier to the balance, thus isolating the fluid sample from the balance. The central elements of the coupling are two magnets, one on each side of a nonmagnetic pressure separating wall made of a beryllium copper alloy. The top magnet, which is an electromagnet with a ferrite core, is hung from the balance (see Figure 1). The lower permanent magnet (together with lifting forks, which pick up the sinkers) is held in stable suspension with

---

Figure 1. Sinkers and magnetic suspension coupling.

respect to the top magnet by means of a feedback control circuit making fine adjustments in the electromagnet current. The magnetic suspension coupling (including a position sensor) is integrated with the measuring cell (pressure vessel) containing the fluid and the sinkers. A mass comparator with a capacity of 111 g and a resolution of 1 μg is used for the weighings.

The temperature of the fluid is measured with a reference-quality 25 ohm capsule-type platinum resistance thermometer (PRT) located in a thermowell attached to the measuring cell. This PRT is read with a resistance bridge referenced to a thermostated standard resistor. Pressures are measured with one of three high-accuracy, vibrating-quartz-crystal pressure transducers; different ranges are used to ensure that any pressure will be within the optimum range of at least one. The transducers and the connecting tubing are thermostated to minimize the influence of ambient temperature.

The thermostat for the measuring cell is a vacuum-insulated cryostat-type design. The measuring cell is surrounded by multiple heated and passive shields which isolate it from ambient. Electric heaters on the cell compensate for the small heat flow from the cell to the slightly cooler shields and allow millikelvin-level control of the cell temperature. Operation at sub-ambient temperatures is effected by circulating a heat-transfer fluid from a chiller through channels in the shield.

Tests were run along either isotherms starting at the highest pressure or pseudo-isochores starting at the lowest temperature. A running average and standard deviation of the temperatures and pressures are computed for the preceding eight readings. When these are within preset tolerances of the set point conditions, a weighing sequence is triggered. The temperatures and pressures are recorded multiple times during a density measurement. Four to eight replicate density determinations are made at each (T,p) state point. The control program then moves to the next temperature on an isochore or prompts the operator to vent the sample to the next pressure on an isotherm. Vapor pressures are measured using a simple static technique. The cell is partially filled with liquid, and the pressure is measured over a range of temperatures.

2.2 Experimental Material

The supplier's specification for the propane was a purity of 99.999 %. Our own analysis by gas chromatography combined with mass spectrometry (MS) and infrared spectrophotometry revealed no impurities on the total ion chromatogram (in MS) or total response chromatogram (in IR). Very small impurity peaks found on the total ion chromatogram were too small to permit identification. The sample was degassed by freezing in liquid nitrogen and evacuating the vapor space. The pressure over the frozen sample was less than 0.003 Pa on the first freeze cycle, indicating that virtually no non-condensible gases were present. The sample used in the densimeter was collected and analyzed again following the measurements; no impurities were detected.

2.3 Measured Data

Propane was measured along 10 isotherms from 265 K to 400 K and along 23 pseudo isochores from 5 kg/m^3 to 487 kg/m^3 with temperatures as high as 500 K. The measured points are indicated in Figure 2. Replicate density determinations were measured at each of the 297 (T,p) state points for a total of 2055 p-ρ-T data. Vapor pressures were measured at 37 temperatures from 270 K to 369 K (0.93 K below the critical temperature); with replicates, these total 209 vapor pressure data points. The data are published elsewhere (McLinden 2005a) and are discussed below with the equation of state.

2.4 Experimental Uncertainties

We claim a very high accuracy for this instrument, and such claims need to be justified. This instrument provides an absolute determination of the density, so it is not sufficient to merely calibrate it against a well-known reference fluid. In fact, this instrument will be used, in the near future, to certify NIST Standard Reference Materials for density, and this imposes the requirement of a rigorous determination of uncertainties and traceability to fundamental SI quantities.

The sinker volumes have been determined at 293.15 K using the hydrostatic comparator technique described by Bowman *et al.* (1974). This method differs from the traditional hydrostatic technique in that the known

density is that of a solid object rather than a reference fluid, such as water. Here we used standards made of single-crystal silicon; their densities were determined and certified by the NIST Mass Group. The uncertainty (k = 2) in the volume difference of the sinkers is 19 ppm. The sinker volume determination at 293 K must be adjusted for temperature and pressure. The temperature dependence of the volumes was based on measured linear thermal expansions of tantalum and titanium. The temperature corrections were further modified using an analysis of low-density gas data; the method is detailed elsewhere (McLinden 2005b).

Figure 2. Experimental p-ρ-T points measured for propane.

The resulting uncertainty in the sinker volume difference is estimated to be 50 ppm at 265 K and 200 ppm at 500 K. The sinker volumes are adjusted for pressure effects using literature values for the bulk modulus. This correction contributes an uncertainty of 50 ppm to the density at 36 MPa.

An automated calibration of the mass comparator is an integral part of each density determination; it is achieved by a mechanism that lowers tare and calibration weights onto a modified balance pan. The weights are fabricated of titanium (tare weight) and stainless steel (calibration weight) with a mass difference of 24.5 g. The different densities of the titanium and stainless steel allow the weights to be nearly identical in volume and surface area. Weighings are made in the order: Ta sinker, Ti sinker, balance calibration weight, balance tare weight, balance tare weight (again), balance calibration weight, Ti sinker, and Ta sinker for a total of eight weighings—two for each object. The weighing design is symmetrical with respect to time, and this will tend to cancel any drift in the temperature or pressure. The weighings are spaced 60 to 90 seconds apart to give adequate time to pick up the next object and allow the magnetic suspension coupling and balance to reach a stable weight. The uncertainty in the calibration weights is estimated to be less than 0.1 mg or 4 ppm of the 24.5 g difference. The linearity of the balance, as specified by the manufacturer, is 3 μg, and the reproducibility is observed to be 2 μg. These uncertainties in the weighings contribute an uncertainty of 0.001 kg/m³ to the fluid density.

The magnetic suspension coupling (MSC) transmits the weight of the sinkers to the balance, and any systematic influence from nearby magnetic materials could seriously affect the density measurement. This is known as a "force transmission error" (Wagner and Kleinrahm 2004). The automated calibration weights allow an analysis of the force transmission error. By weighing the sinkers in vacuum (using the MSC) and comparing this measurement to the known mass of the sinkers, the force transmission error is obtained:

$$\varepsilon_{\text{FTE}} = W[\text{fork}+\text{sinker}] - \left\{ W[\text{fork}+\text{cal wt}] + V_{\text{cal wt}}\rho_{\text{air}} \right\} - \left(m_{\text{sinker}} - m_{\text{cal wt}} \right), \tag{2}$$

where W refers to the balance reading for the weighing of the objects inside the bracket. The $V\rho$ term is needed to correct for air buoyancy on the calibration weight. Based on an analysis of several hundred vacuum weighings carried out over the course of six months, the average error is 0.915 mg with σ = 0.078 mg. This is equivalent to 15.2 ppm of the 60 g sinker mass with σ = 1.3 ppm. The effect of temperature over the range 250 K to 500 K is less than 2 ppm. The force transmission errors for the two sinkers are within 1 ppm of each other. Assuming that the error is linear with the difference in the loading on the MSC would result in a constant relative error in density of 15.2 ppm. We have not made any correction for the force transmission error pending further study of the effect, but have added 15.2 ppm to the uncertainty in density. The magnetic properties of the test fluid itself can lead to another source of systematic error in the MSC as discussed by Wagner and Kleinrahm (2004), but propane is nearly nonmagnetic and the two-sinker technique nearly cancels any error so this "fluid-specific effect" should be very small for the results presented here.

The overall uncertainty (k = 2) in the density varies smoothly between (0.0050 % + 0.001 kg/m³) at 265 K, (0.0025 % + 0.001 kg/m³) at 293 K, and (0.02 % + 0.001 kg/m³) at 500 K. The effect of pressure adds an additional uncertainty varying from near zero at ambient pressure to 0.0050 % at 36 MPa.

The PRT used to measure the temperature of the fluid was calibrated from 83 K to 505 K with fixed point cells (argon triple point, mercury triple point, water triple point, indium freezing point and tin freezing point). This was done as a system calibration, meaning that the PRT was removed from its thermowell in the measuring cell and inserted into a fixed point cell using the same resistance bridge, standard resistor, and lead wires as were used in the measurements. The uncertainty in the temperature, including possible temperature gradients, is 4 mK.
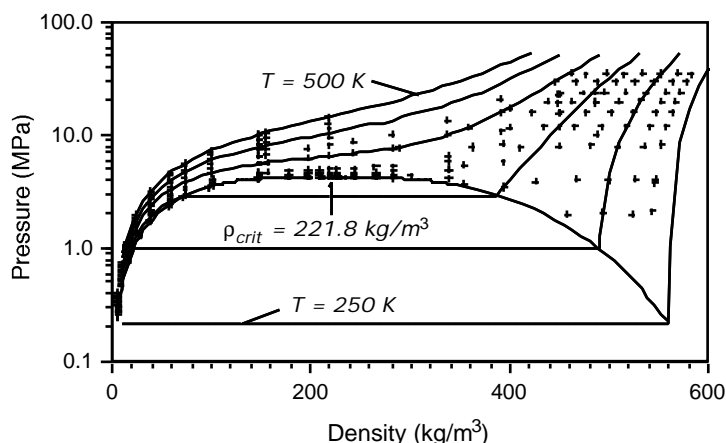
The pressure transducers were calibrated with piston gages. A gas-operated system was used for pressures up to 7 MPa and a hybrid gas/oil system is used for pressures up to 40 MPa. These calibrations were done *in-situ* by connecting the piston gage to the sample port of the filling manifold. Based on the uncertainties for the piston gages, the repeatability observed for these transducers, and the uncertainties associated with the hydrostatic head correction, we estimate the total ($k = 2$) uncertainty in pressure to be (0.0017 % + 0.000065 MPa) for $p < 1.3$ MPa; (0.0032 % + 0.00034 MPa) for $p < 6.8$ MPa, and (0.0051 % + 0.002 MPa) for $p < 40$ MPa.

3. EQUATION OF STATE

An equation of state (EOS) is a mathematical description of the thermodynamic properties of a fluid. A properly formulated EOS will describe all of the thermodynamic properties, including those that cannot be measured directly, in a thermodynamically consistent way. An equation of state is, thus, the final output of our work on the properties of a given fluid, and it is the most efficient way to provide property data to engineers working in the refrigeration or chemical process industries.

Equations of state have taken countless different forms. The most familar are those expressing pressure as a function of temperture and density, such as the ideal-gas law $p = RT/\rho$. But most modern, high-accuracy equations are written in terms of the reduced molar Helmholtz free energy as a function of temperature and density, and we adopt that form here. The equation is composed of separate terms arising from ideal-gas behavior (superscript id) and a "residual" or "real-fluid" (superscript r) contribution:

$$\phi = \frac{A}{RT} = \phi^{\text{id}} + \phi^{\text{r}} , \qquad (3)$$

where R is the gas constant and T is the absolute temperature. The residual contribution is given by

$$\phi^{\text{r}} = \sum_k N_k \tau^{t_k} \delta^{d_k} \exp\left[-\alpha_k \left(\delta - \varepsilon_k\right)^{l_k}\right] \exp\left[-\beta_k \left(\tau - \gamma_k\right)^{m_k}\right] , \qquad (4)$$

where the temperature and density are expressed in the dimensionless variables $\tau = T^*/T$ and $\delta = \rho/\rho^*$, where T^* and ρ^* are reducing parameters that are often equal to the critical parameters. The N_k are numerical coefficients fitted to experimental data. The multipliers α_k and β_k and exponents t_k, d_k, l_k, and m_k are optimized for a particular fluid or group of fluids. The ideal-gas contribution is represented in terms of the heat capacity of the ideal-gas state. A major advantage of this form is that all the other thermodynamic properties can be expressed using only derivatives of Equations 3 and 4. Lemmon and Jacobsen (2005) describe the Helmholtz energy equation of state in detail and give the numerical coefficients in Equation 4; this reference also describes the calculation of all the thermodynamic properties from the Helmholtz energy.

The parameters ε_k and γ_k appearing in Equation 4 are relatively new extensions of the traditional Helmholtz equation of state form and have been fitted for only a few fluids, including R125, carbon dioxide, nitrogen, and water. Lemmon and Jacobsen (2005) describe the techniques used in developing the R125 equation. These new terms improve the fit of caloric properties in the critical region. New nonlinear fitting techniques allow extrapolation beyond the range of the data, and provide a more physically reasonable behavior of the equation inside the two-phase region. The Helmholtz EOS is generally empirical, but it is designed to exhibit proper limiting behavior in the ideal gas and low density regions and to extrapolate to temperatures and pressures higher than those experimentally measured.

3.1 Fitting Techniques

The development of the equation of state is a process of correlating selected experimental data to a model. The selected data are usually a subset of the available database determined by the correlator to be representative of the most accurate values measured. In all cases, experimental data are considered paramount, and the validity of any equation of state is evidenced by its ability to represent the thermodynamic properties of the fluid within the uncertainty of the experimental values. Secondary tests of validity are the ability to extrapolate outside the range of experimental data and the ability to represent properties that were not measured, such as entropy.

Fitting can use techniques that are either linear or nonlinear in the parameters. Linear fitting (*i.e.*, linear least squares regression) is much simpler and will yield the parameters to a given model directly, without iteration. Nonlinear techniques are more computationally intensive, but are also much more powerful. For example, linear fitting of Equation 4 requires finding the best combination of the exponents of temperature and density in the summation, usually starting with a fixed "bank of terms," only then are the the the N_k, α_k, and β_k determined. In contrast, nonlinear techniques can simultaneously fit both the coefficients that are simple multipliers (the N_k, α_k, and β_k in Equation 4) and coefficients that are exponents (t_k, d_k, l_k, and m_k).

An additional advantage of nonlinear fitting is the ability to fit experimental data using virtually any measured property. For example, in linear fitting of the speed of sound, preliminary equations are required to

transform the measured pressure and temperature to the independent variables of density and temperature required by the equation of state. Additionally, the ratio C_p/C_v (also from a preliminary equation) is required for a linear fit of the sound speed. Nonlinear fitting can use pressure-temperature-sound speed data directly without any transformation of the input variables. Another advantage in nonlinear fitting is the ability to use "greater than" or "less than" operators, to control the extrapolation behavior of properties such as heat capacities to low or high temperatures. In linear fitting, only equalities are typically used. This often requires the correlator to extrapolate data to generate "data points" where no experimental data exist; these are then put into the fit with low weight to constrain the fit to have the proper behavior. This is most often done for heat capacity and/or speed of sound. With successive fitting, the curves are updated until the correlator is content with the final shape. In nonlinear fitting, curves can be controlled to ensure that a calculated value along a constant property path is always greater (or less) than a previous value; thus magnitudes are not specified, only the shape. The nonlinear fitting algorithm determines the best magnitude for the properties based on other information.

In this work, we use nonlinear fitting techniques. A small subset of data was used in the fit due to the extensive iterative calculations required to develop the equation. The data were selected from the p-ρ-T, C_{sat}, vapor pressure, and sound speed data discussed below. The resulting equation was compared to all the experimental data to verify that the data selection was sufficient to allow an accurate representation of the available data. A nonlinear fit requires initial guesses for both the coefficients and exponents. We started with the EOS for R125 (Lemmon and Jacobsen, 2005). The nonlinear algorithm adjusted the parameters of the equation of state to minimize the overall sum of squares of the deviations of calculated properties from the input data, where the residual sum of squares was represented as

$$S = \sum W_\rho F_\rho^2 + \sum W_p F_p^2 + \sum W_w F_w^2 + \cdots, \tag{5}$$

where W is the weight assigned to each data point and F is the function used to minimize the deviations. The equation of state was fitted to p-ρ-T data using deviations in pressure $F_p = (p_{\text{data}} - p_{\text{calc}})/p_{\text{data}}$ for vapor phase and critical region data, and deviations in density, $F_\rho = (\rho_{\text{data}} - \rho_{\text{calc}})/\rho_{\text{data}}$, for liquid phase data. Other experimental data were fitted in a like manner, e.g., $F_w = (w_{\text{data}} - w_{\text{calc}})/w_{\text{data}}$ for the speed of sound. The weight for each selected data point was individually adjusted according to type, region, and uncertainty.
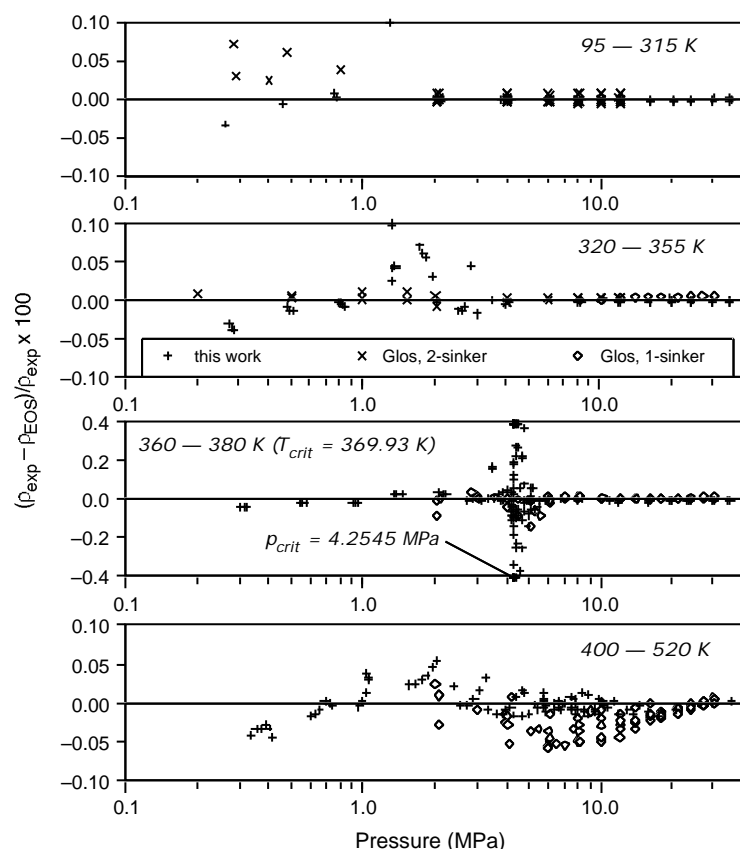
We apply a number of constraints to give the equation the proper behavior; these are discussed in detail elsewhere (Lemmon and Jacobsen 2005 and Lemmon et al. 2005). The exponents on density in the equation of state must be positive integers so that the derivatives of the Helmholtz energy with respect to density have the correct theoretical expansion around the ideal gas limit. Since nonlinear fitting typically results in noninteger values for the density exponents, it is necessary to round each density exponent to the nearest integer, then refit all the other parameters to minimize the overall sum of squares. This process was repeated until all the density exponents in the final form were integers. A similar process was used for the temperature exponents to reduce the number of significant figures to one or two past the decimal point. The exponents on temperature must be positive to avoid problems in the high-temperature region. The values of the first and second derivatives of pressure with respect to density were constrained to zero at the critical point.

The end result is an equation of state that fits the experimental data better and has fewer terms than an equation developed with the traditional linear fitting techniques. The new EOS has 24 terms. In addition to being computationally simpler, an equation with fewer terms generally exhibits better extrapolation behavior compared to a longer EOS. In the longer equations, two or more correlated terms are often needed to approximate the accuracy of a single term in the nonlinear fit. The values of these correlated terms are often large in magnitude, and the behavior of the equation outside its range of validity is often unrealistic.

3.2 Comparisons to Data

Figure 3 shows comparisons of densities calculated with the new equation of state (Lemmon et al. 2005) to experimental data. Experimental p-ρ-T data are the most important data for the fitting of the EOS. The most comprehensive and accurate data are those of Glos et al. (2004) and the present work. Glos et al. used a two-sinker densimeter; they also report an independent set by Claus using a single-sinker densimeter. For the compressed liquid region, the EOS represents every data point of Glos between 90 K (the lower limit of the data) and 240 K with deviations less than 0.01% in density. From 240 K to the upper limit of the Glos data at 340 K there are only seven data points with deviations greater than 0.01% in density. The present data are extraordinarily consistent with the Glos data, and are all fit to within 0.01 % at temperatures up to 360 K. The overlapping single-sinker data of Claus in this region are also very consistent. For temperatures from 380 K to 500 K, the present data are fit within 0.02 % for pressures above 6 MPa. At these higher temperatures, the data of Claus show small systematic deviations with the present data and equation of state of up to 0.06 %.

The vapor-phase p-ρ-T data show larger deviations compared to the liquid-phase, but all of the points from 0.2 to 4.25 MPa are fitted within 0.085 % except for two points at 0.12 % and 0.16 %. (Points with deviations larger than the plot limits are drawn on the plot frame.) At the lowest pressure of 0.3 MPa measured in the

Figure 3. Comparison of the equation of state with experimental *p*-ρ-*T* data.

present work the density is only 5 kg/m³, and this is at the lower limit of the apparatus. At these low pressures, priority in the fitting is given to correctly approaching the ideal-gas limit rather than attempting to fit data that may be subject to systematic errors.

In the critical region, the deviations are higher. This is expected, due both to fitting the critical region with an analytical equation of state, and to experimental difficulties (small changes in temperature or pressure can result in large changes in density). Nevertheless, the present data (which include points within 0.1 K of the critical temperature and 5 % of the critical density) are generally fitted within 0.4 % for temperatures between 360 K and 380 K and pressures between 4.25 MPa to 6 MPa, although several points within 1 K of the critical temperature have larger deviations. The near-critical data of Claus show similar deviations. Deviations in pressure are perhaps more useful in the critical region than the deviations in density shown here. In the critical region, the deviations in pressure are all less than 0.05 %.

Vapor-phase speed of sound data were the primary data used in fitting the ideal-gas part of the equation of state. These data are all fitted within 0.04 % as shown in Figure 4. Two high-accuracy data sets are available for the speed of sound in the liquid; these extend from near the triple point to 320 K. The calculation of speed of sound involves several first and second derivatives of the Helmholtz energy, and thus sound speed data are a powerful consistency check on the equation of state. The uncertainty in these data are about 0.1 %, and the equation of state represents nearly all of these data to within this uncertainty as shown in Figure 4.

The *p*-ρ-*T* and sound speed data discussed above are single-phase data. In principle, these would be sufficient to fit the equation of state, but, in practice, additional data are needed to constrain the saturation boundary. Vapor pressures and saturation heat capacities are the most useful. Figure 5 compares vapor pressures calculated with the equation of state to experimental data. The data of Glos *et al.* (2004) extend from 110 K to 340 K and

were the primary vapor pressures used. They are fitted within 0.01 % at temperatures above 180 K. The deviations increase to 1 % at 130 K. The two points at 110 K and 120 K deviate by substantially more. However, the pressures at the lowest temperatures are extremely small (0.6 Pa at 110 K) and at such low pressures, experimental uncertainties in vapor pressure are large. The vapor pressures measured in the present work extend from 270 K to near the critical temperature. They were used from 340 K to 369 K where they are fit within 0.02 %. These data show systematic deviations of up to 0.05 %
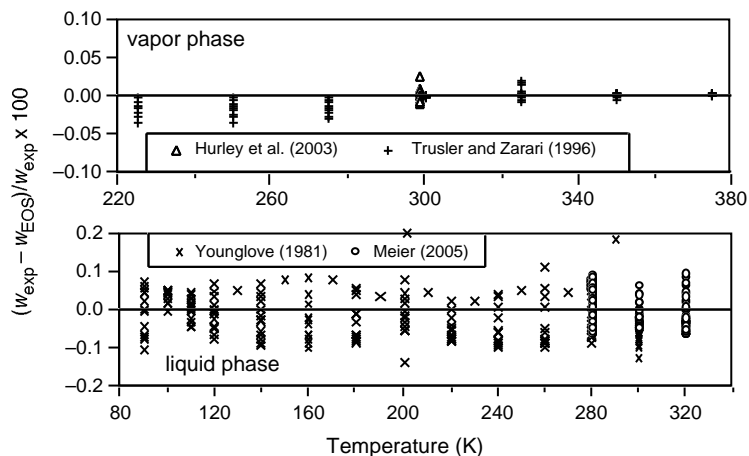

Figure 4. Comparison of the equation of state with sound speed data.

compared to the Glos data. Because of these systematic differences, both sets could not be fit simultaneously, and the data of Glos were used below 340 K because of their wider temperature range.

Saturation heat capacities C_{sat} were measured by Perkins (2005) as part of this project. (The saturation heat capacity is the change in energy per unit temperature for the liquid along the saturation boundary. It is given by $T[\partial s/\partial T]$ and is measured with an isochoric (constant volume) calorimeter filled with a two-phase sample. C_{sat} is nearly the same as C_p at pressures below about 0.1 MPa.) Deviations of these data (shown in Figure 5) are no more than 0.5 % from

Figure 5 Comparison of the equation of state with saturation data.

the triple point temperature of 85.523 K (Pavese and Besley 1981) to 265 K. The deviations increase to as much as 1 % at temperatures up to 320 K. These deviations are comparable to the experimental uncertainties. At higher temperatures, corrections for the vaporization of a portion of the liquid increase the uncertainties. These data are in good agreement with the data of Goodwin (1978).

The critical point of propane has been directly measured, but the uncertainties in the experimental values are relatively large compared to those of other well-studied fluids, such as carbon dioxide. The best measurements of the critical temperature, pressure, and density range from 369.88 K to 369.94 K, 4.254 MPa to 4.26 MPa, and 4.98 mol/L to 5.0 mol/L. The critical parameters can also be deduced directly from the fit of the equation of state. We measured extensive p-ρ-T data in the near-critical region (see Figure 2), and these give fitted critical parameters with uncertainties comparable to the experimental values. Our values are 369.93 K, 4.2545 MPa, and 5.03 mol/L. The fitted critical parameters are completely consistent with the equation of state, and this is a significant advantage. Constraining the fit to experimental critical parameters can distort the thermodynamic surface in the near-critical region.

The above discussion has covered only the most accurate data. These represent only a small fraction of the data available for propane. The data include 42 references totaling 4855 p-ρ-T data, more than 1100 vapor pressure data points from 66 references, 13 sources with 334 points for heat capacity data, and 11 references with 1050 data points for speed of sound. A full discussion of all the data is presented in Lemmon $et\ al.$ (2005).

3.3 Extrapolation Behavior

It is not sufficient for an equation of state merely to represent the experimental data. It should also extrapolate reliably outside the range of measured data. Propane is a common reference fluid for other fluids in extended corresponding states (ECS) models. In this application, the reduced temperature and pressure of the fluid modeled with ECS may correspond to high or low temperatures or pressures or may be inside the 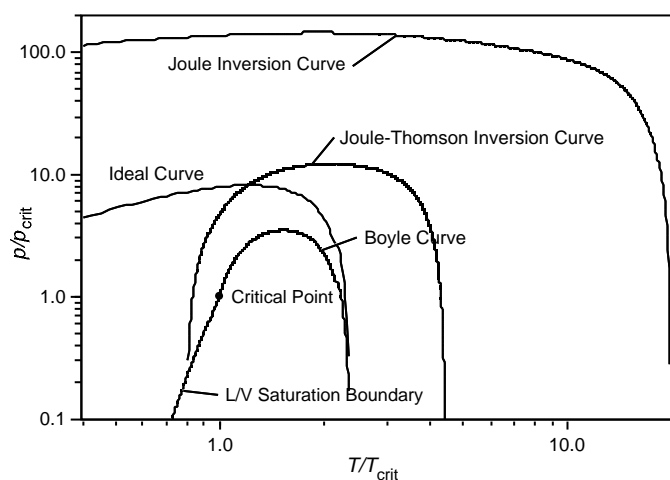two-phase region for the reference fluid. Thermodynamic calculations often require iterations that may stray to extreme values before they converge.

One indication of the extrapolation behavior of an EOS are the locations of several characteristic curves on pressure-temperture coordinates, as shown in Figure 6. The "ideal curve" is the locus of points where the ideal gas law is satisfied $Z = p/RT\rho = 1$. The Boyle curve is given by $(\partial Z/\partial V)_T = 0$. The Joule-Thomsom inversion curve is where $(\partial Z/\partial T)_p = 0$. The Joule inversion curve is $(\partial Z/\partial T)_V = 0$. These curves fall in roughly the same locations on reduced coordinates for nearly all fluids, and the

Figure 6. Characteristic curves calculated with the new equation of state.

present equation of state reproduces the expected behavior. The curves should all be smooth and continuous. Many examples exist of equations of state that accurately represent the experimental data but display odd bumps and inflections where the curves lie outside the range of the data. Finally note that the present EOS displays reasonable behavior to at least a reduced temperture $T/T_{crit}= 20$ and reduced pressure $p/p_{crit} = 200$, corrresponding to 7400 K and 850 MPa.

4. DISCUSSION AND CONCLUSIONS

New p-ρ-T measurements combined with other data have been used to develop a new equation of state for the thermodynamic properties of propane. The equation fits a variety of data types within their experimental uncertainties. The fit of the p-ρ-T data, in particular, is among the best for any fluid. The new EOS will serve as the reference fluid in modeling other fluids (with limited data) using extended corresponding states methods. It will also be used in the development of "short form" equations of state. The fitting techniques used in developing the equation of state define the new state of the art.

5. ACKNOWLEDGEMENTS

REFERENCES

Bowman, H.A., Schnoover, R.M. and Carroll, C.L. (1974). The utilization of solid objects as reference standards in density measurements. *Metrologia* **10**: 117-121.

Glos, S., Kleinrahm, R. and Wagner, W. (2004). Measurement of the (p,ρ,T) relation of propane, propylene, n-butane, and isobutane in the temperature range from (95 to 340) K at pressures up to 12 MPa using an accurate two-sinker densimeter. *J. Chem. Thermodynamics* **36**: 1037-1059.

Goodwin, R.D. (1978). Specific heats of saturated and compressed liquid propane. *J. Res. Natl. Bur. Stand.* **83**:449-458.

Hurly, J.J., Gillis, K.A., Mehl, J.B. and Moldover, M.R. (2003). The viscosity of seven gases measured with a Greenspan viscometer. *Int. J. Thermophysics* **24**: 1441-1474.

Lemmon, E.W. and Jacobsen, R.T. (2005). A new functional form and fitting techniques for equations of state with application to pentafluoroethane (HFC-125). *J. Phys. Chem. Ref. Data* **34**: 69-108.

Lemmon, E.W., McLinden, M.O., and Wagner, W. (2005). Thermodynamic properties of propane. III. Equation of state. *J. Chem. Eng. Data* (submitted for publication).

McLinden, M.O. (2005a). Thermodynamic properties of propane. I. p-ρ-T behavior from 265 K to 500 K with pressures to 36 MPa. *J. Chem. Eng. Data* (submitted for publication).

McLinden, M.O. (2005b). Densimetry for primary temperature metrology and a method for the in-situ determination of densimeter sinker volumes (manuscript in preparation).

McLinden, M.O. and Lösch, C. (2005). Apparatus for wide-ranging, high-accuracy fluid p-ρ-T measurements based on a compact two-sinker densimeter. *J. Chem. Eng. Data* (submitted for publication).

Meier, K. (2005). Helmut Schmidt Universität, Hamburg, Germany, personal communication.

Miyamoto, H. and Watanabe, K. (2000). A thermodynamic property model for fluid-phase propane. *Int. J. Thermophysics* **21**: 1045-1072.

Pavese, F. and Besley, L.M. (1981). Triple-point temperature of propane: Measurements on two solid-to-liquid transitions and one solid-to-solid transition. *J. Chem. Thermodynamics* **13**: 1095-1104.

Perkins, R.A., Sanchez Ochoa, J.C. and Magee, J.W. (2005). Thermodynamic properties of propane. II. Specific heat capacity at constant volume from 85 K to 345 K with pressures to 35 MPa. *J. Chem. Eng. Data* (submitted for publication).

Trusler, J.P.M. and Zarari, M.P. (1996). The speed of sound in gaseous propane at temperatures between 225 K and 375 K and at pressures up to 0.8 MPa. *J. Chem. Thermodynamics* **28**: 329-335.

Wagner, W. and Kleinrahm, R. (2004). Densimeters for very accurate density measurements of fluids over large ranges of temperature, pressure, and density. *Metrologia* **41**: 24-39.

Younglove, B.A. and Ely, J.F. (1987). Thermophysical properties of fluids. II. Methane, ethane, propane, isobutane and normal butane. *J. Phys. Chem. Ref. Data* **16**: 577-798.

Younglove, B.A. (1981). Velocity of sound in liquid propane. *J. Res. Natl. Bur. Stand.* **86**: 165-170.